Supplementary Materials

1. OVERVIEW OF THE STUDY REGION

China covers a total of 9.6 million square kilometers. Its geomorphology is extremely complex, and there are three terrain steps from Qinghai-Tibetan Plateau (averaged elevations > 4000 m, dominated by grassland), to the Kunlun Mountains (elevation ranges 1000-2000 m), and the eastern hills and plains (mostly below 500 m from the average sea level). The latter region can be characterized with intensive agricultural/anthropogenic activities (Fig.1). There were 2,554 (in 2015) and 2,693 (in 2020) natural lakes (surface area > 1 km^2) distributed across China, respectively (National Tibetan Plateau Data Centre) [19] (Figure S1). Chinese lake densities vary across the country. We used five lake zones as defined by Wang and Dou (1998, Early National Investigation) [34]. The lakes in the ELR draw great attention because over 50% of the Chinese population is living there, and many lakes serve critical ecological functions. The TQR lakes grow or disappear fast depending on the supply from snow and ice melt [19]. Due to high elevations and aquatic habitats essentially undisturbed by human activity, lakes in this region are mostly oligotrophic with high water clarity. The region is sensitive to global warming [57]. In the MXR, the numbers of lakes decreased in recent years. The other lake regions (YGR, ELR and NLR) are external drainage systems in the Asian monsoon climate region. The YGR is located in the southwest of China, and karst topography dominated the landscapes. Owing to the long residence time of water and to intensive human activities, many lakes in YGR are supplied from eutrophic sources and experience black and odorous algal blooms. The majority of NLR lakes were found on the Songnen Plain, with the remainder in the mountainous regions. In the ELR, there were many lakes in the floodplains of the middle and lower Yellow, Yangtze, and Hai Rivers.

2. METHODS

2.1. In situ water quality collection and field measurements

Some lakes were visited frequently and some were sampled only once. Bulk samples were taken from the middle of lakes, approximately 0.5 m below the surface, as often as possible. They were immediately stored in 1L amber high-density polyethylene bottles that had been pre-rinsed with field samples, and kept at 4℃ in a refrigerator powered. A multi-parameter water quality probe (YSI 6600, USA) was also used to determine the pH and electrical conductivity (EC, μs cm^{-1}). A black-and-white disk was used to measure the Secchi disk depth (SDD, m).

2.2. Water quality and light absorption determination in laboratory

A standard turbidity solution was made in the laboratory (20 ± 2 °C) from artificial turbid water with 400 NTU by mixing (N_2H_4) H_2SO_4 and $(CH_2)_6N_4$, and a blank sample (distilled water filtered through 0.2 glass fiber membranes) was prepared. On a UV-VIS spectrophotometer (SHIMADZU UV-2600, Japan), the absorbance curve of the standard solution (0, 4, 10, 20, 40, 80, and 100 NTU) at 680 nm was utilized as a calibration curve to get measured water turbidity of lake samples. In addition, the transferred bulk samples were immediately filtered via 0.45-μm Whatman cellulose acetate membrane filters. These filters were first pre-soaked with 90% acetone solution at 0℃ for 24 h in the dark. Using a UV-2660PC spectrophotometer (Shimadu, Kyoto, Japan) at four wavelengths (750, 663, 645 and 630 nm) in line with SCOR-UNESCO equations [58], the Chl-a concentrations (Chl-a, μg L^{-1}) were determined. To retain suspended particles, the bulk samples were also filtered again via 0.45-m Whatman cellulose acetate membrane filters. The suspended matter (SPM, mg L^{-1}) concentration was determined gravimetrically.

The absorption coefficients of optical active substances were CDOM absorption coefficient $a_{CDOM}(\lambda)$ and total particulate matter $a(\lambda)$, and the latter can be separated into

phytoplankton pigment absorption coefficient $a_{ph}(\lambda)$ and non-algal particles absorption coefficient $a_d(\lambda)$ [36,56,59]. Finally, $a_{ph}(\lambda)$ was calculated by subtracting $a_d(\lambda)$ from $a_P(\lambda)$. The CDOM samples were acquired using the 0.22 μm Whatman Nuclepore filters, and then scanned in 200-800 nm equipped with a 1 cm quartz cuvette on a Shimazdu UV-2660PC spectrophotometer. More details can be found in previous studies [31-32,49]. We used absorption values at 443 nm to characterize the amount of CDOM - $a_{CDOM}(443)$.

2.3. MSI imagery match-ups

Sentinel-2 satellites (Sentinel-2A and -2B) with the MSI sensor were launched in 2015, with the aim to monitor the full Earth.The MSI Level-1C imgery, 100×100 km^2 ortho-images in UTM/WGS84, can be downloaded for free from the European Space Agency's website, and have a revisit time of about 5-10 days. There were thirteen spectral bands ranging from 443 nm to 2190 nm, with spatial resolutions are 10 m, 20 m and 60 m. C2RCC processor can remove atmospheric signals consistent with earlier studies by Warren et al., (2021)[37], Pahlevan et al., (2019) [17] and Li et al., (2021, 2022)[16,33], which found that C2RCC has the best performance for qualifying water qualities. MSI revisit time in high latitude areas is about 1-2 days because there are two Sentinel-2's in space and their orbits overlap close to the poles [15]. However, in low latitude regions, there are less frequent revisit times [16]. It is accepted that turbidity is relatively stable for comparison between remote sensing and field surveys if there are no rainfall events or hydrological variations and the two sampling events occur within 7 days of each other [49].

2.4. Data on abiotic factors

The averaged depths and lake volume in millions of cubic meters were gathered from Hydrosheds datasets which were estimated using the geo-statistical modeling approach of Messager et al. (2016) [16]. Hydrosheds datasets can be found in website https:// developers.google.cn/earth-engine/datasets/tags/hydrosheds. Elevation (30 m) was determined from the DEM/SRTM of the Shuttle Radar Topography Mission (earthdata.nasa.gov). The annual mean wind speed recording as m s^{-1} of east wind approximately 10m above the surface of lakes was extracted from the European Centre for Medium-Range Weather Forecasts (ECMWF, www.ecmwf.int). Likewise, the annual temperature (°C), precipitation (mm), normalized difference vegetation index (NDVI), GDP and population data were sourced from the Resource and Environmental Science and Data Center (https://www.resdc.cn/).

2.5. Chinese turbidity products and lake masks

The lake boundaries (1960s-2020) were extracted using Landsat images from mid-late summer and early fall due to the low cloud contamination and stable water qualities [14,49]. However, for achieving more accurate lake boundaries, we also retrieved them from MSI fall images. We used Modified Normalized Difference Water Index (MNDWI), density slicing, Tasseled Cap Transformation (TC) with a multi-threshold approach based on decision trees to classify satellite images into two water and non-water sections [49]. To avoid the influence of lake bottoms, helophytes, and emergent vegetation in shallow coastal areas, the lake masks were buffered by 3-10 water pixels (30-300 m) in ArcGIS 10.2 (Esri Inc. Redlands, CA, USA). This process depended on the area and length/width ratio of lakes. In addition, we used NDVI (normalized difference vegetation index) to remove algal bloom areas from every MSI scene. The NDVI was based on Band 4, Band 8 and Band 12. The NDVI thresholds changed with different scenes, and the ranges were 0.20 to 0.70 [11]. The obtained lake boundaries were used in the turbidity analysis.

2.6. Statistical analyses and accuracy assessment

Statistical analyses, e.g., regression and correlation analyses, were conducted to examine the relationships between water qualities variables (Chl-a, SDD, SPM and turbidi-

ty, etc.) among lakes. The *r* and R^2 were computed to determine the correlation coefficient and regression coefficient, respectively. The development and performance of our turbidity models were evaluated by fitting R^2 and the slope between measured- and estimated- turbidity, and the errors such as root mean square error (RMSE) and the mean absolute errors (MAE), respectively. Briefly, the model had high concordance (high R^2 and slope close to 1) and low error rate for estimating turbidity.

Table S1. Field surveys of lake name, abbreviation, location, and sampling dates of *in situ* lakes across China. Time is sampling date; *N* denotes numbers of samples. + means brackish lake.

Lakes	Abb.	Location(N/E)	Time [a]	*N*	Lakes	Abb.	Location(N/E)	Time [a]	*N*
Yueliang Pao	YLP(1)	45°43', 123°59'	2018-10	6	CuoNa	CN(33)	32°03',91°27'	2017-08	5
Qingnian	QN(2)	45°40',131°49'	2017-06	3	SeLinCo	SLC(34)	31°49',89°11'	2017-08	4
XiaoXingKai-Hu	XXKH(3)	45°22',132°22'	2018-07	11	ChaoHu	CH(35)	31°41',117°23'	2019-04	9
			2018-10	9	BaMuCuo	BMC(36)	31°32', 90°34'	2017-08	2
DaXingKaiHu	DXKH(4)	45°10',132°25''	2018-10	19	TaRuoCo	TRC(37)	31°07',84°17'	2017-08	4
XinMiaoPao	XMP(5)	45°10',124°27'	2018-10	6	ZhaRiNanMuCo	ZRNM(38)	31°00',85°31'	2017-08	4
TaiPingChi	TPC(6)	44°02',124°57'	2018-06	3	NamoCo	NMC(39)	30°47',90°51'	2017-08	2
XingXingShao	XXS(7)	43°37',126°3''	2018-10	4	PoYang	PY(40)	29°41',116°10'	2019-04	9
DaLi	DL(8)	43°17',116°35'	2019-07	19				2019-07	9
ErlongLake	EL(9)	43°14',124°50'	2018-07	10	ZheLin	ZL(41)	29°14',115°28'	2019-07	7
HongShan	HS(10)	42°43',119°41'	2017-04	4				2019-11	4
			2019-07	5	GuTian	GT(42)	26°36',118°48'	2017-06	4
QingHe	QH(11)	42°32',124°12'	2018-10	4	FengShuBa	FSB(43)	24°27',115°23'	2019-04	2
BaiShan	BS(12)	42°37',127°08'	2019-06	6	YangXi	YX(44)	23°55',116°52'	2017-07	3
YunFeng	YF(13)	41°33',126°35'	2018-10	1	XinFengJiang	XFJ(45)	23°50',114°35'	2019-01	5
GuanYinGe	GYG(14)	41°22',124°18'	2018-10	5				2019-04	6
HengLong	HL (15)	41°19',125°28'	2018-10	9				2019-11	7
WuLiang-SuHai	WLSH(16)	40°54',108°52'	2019-08	10				2017-07	1
DaiHai	DH(17)	40°33',112°41'	2017-04	2	BaiPenZhu	BPZ(46)	23°06',115°08'	2019-04	5
			2019-08	8				2019-07	3
HaLa	HL(18)	38°12',97°35'	2019-09	1				2019-11	6
FenHe	FH(19)	38°04',111°53'	2017-04	3	DaGuangBa	DGB(47)	18°57',109°0'	2017-07	1
KeLuKe	KLK(20)	37°15',96°54'	2017-08	8	XiangYunQing-Hai	XYQH(48)	25°26',100°36'	2017-07	2
			2019-09	2	HunShuiHai	HSH(49)	25°32',100°36'	2017-07	3
TuoSu	TS(21)	37°10',96°54'	2017-08	10	Er'Hai	EH (50)	25°54',100°09'	2017-07	3
QingHaiHu	QHH(22)	36°57',100°21'	2019-09	32	XiHu	XH(51)	26°01', 100°02'	2017-07	3
LiJiaXia	LJX(23)	36°07',101°47'	2017-09	4	ChengHai	CH(52)	26°33', 100°39'	2017-07	3
			2019-09	13	ChangQiaoHai	CQH(53)	23°26', 103°20'	2017-07	4
LongYangXia	LYX(24)	36°09',100°48'	2019-09	7	QiongHai	QH(54)	27°49', 102°19'	2018-08	4
LiuJiaXia	LJX(25)	35°51',103°15'	2017-09	8	YiHai	YH(55)	28°43', 102°14'	2018-08	1
			2019-09	11	CuoNiBa	CNB(56)	30°18', 99°33'	2018-08	1
XiaoLangDi	XLD(26)	34°56',112°18'	2019-09	19	DangZiCuo	DZC(57)	32°04', 98°55'	2018-08	2
WeiShan	WS(27)	34°38',117°18'	2019-01	6	Ang'Cuo	AC(58)	32°00', 99°00'	2018-08	2
LuoMa	LM(28)	34°06',118°13'	2019-04	7	XinLuHai	XLH(59)	31°51', 99°07'	2018-08	1
HongZe	HZ(29)	33°06',118°43'	2019-01	10	SanChaHu	SCH(60)	30°18', 104°16'	2018-08	4
			2019-04	2	MaHu	MH(61)	28°24', 103°46'	2018-08	3
			2019-08	3	GuiZhouCaoHai	GZCH(62)	26°50', 104°15'	2018-04	3
			2019-11	8				2018-08	1

GaoYou	GY(30)	32°48',119°18'	2019-01	10	BaiLang	BL(63)	25°48', 103°52'	2018-04	2
			2019-04	5				2018-08	2
			2019-11	10	HuaShan	HS(64)	25°47', 103°54'	2018-04	3
XiBa	XB(31)	25°38',104°04'	2018-04	1	PianQiao	PQ(65)	25°58', 103°55'	2018-04	2
XiHe	XH(32)	25°34',103°42'	2018-04	1	XiangZongHai	XZH(66)	25°05', 103°52'	2018-04	2

[a] The time is Year-month; [+] means brackish lake.

Table S2. ANOVA analysis of reflectance spectra *rhown*(λ) according to OWTs (Avg.± SD.).

Wavelength (nm)	OWT C1 (*N*=115)	OWT C2 (*N*=245)	OWT C3 (*N*=124)	*F*	*p*
443	0.0273±0.012	0.0105±0.007	0.0323±0.0063	346.24	0.000 **
492	0.0394±0.013	0.0158±0.009	0.0493±0.0083	542.15	0.000 **
560	0.0583±0.018	0.0216±0.009	0.0989±0.0172	1314.49	0.000 **
665	0.0204±0.013	0.0069±0.0050	0.0662±0.0130	1530.54	0.000 **
704	0.0163±0.016	0.0052±0.0045	0.0653±0.0143	1507.36	0.000 **
740	0.0048±0.0043	0.0015±0.0014	0.0231±0.0058	1401.00	0.000 **

** $p < 0.01$.

Table S3. Environmental abiotic factors in China.

	Parameters	Data format	Resolution	Time	Sources	References
Lake characteristic factors	Lake area	shape	30m	2015, 2020	National Tibetan Plateau Data Centre	Zhang et al. (2019)
	Lake volume	shape	-	-	Hydrosheds datasets	Messager et al. (2016
	The average lake depth	shape	-	-	Hydrosheds datasets	Messager et al. (2016)
Natural factors	Elevation	Raster	30m	-	DEM/SRTM of the Shuttle Radar Topography, NASA	-
	Annual mean wind speed	Raster	-	2015, 2020	European Centre for Medium-Range Weather Forecasts	-
	normalized difference vegetation index (NDVI)	Raster	1km	2020	Resource and Environmental Science and Data Center	-
	Annual temperature	Raster	1km	2020	Resource and Environmental Science and Data Center	-
	Annual precipitation	Raster	1km	2020	Resource and Environmental Science and Data Center	-
Anthropogenic factors	Gross Domestic Product	Raster	1km	2019	Resource and Environmental Science and Data Center	-
	Populations	Raster	1km	2019	Resource and Environmental Science and Data Center	-

Table S4. Pearson analysis of water quality parameters from in situ lakes across China.

Parameters	pH	EC	Turbidity	SDD	SPM	Chl-a	TN	TP	a(443)	a_{ph}(443)	a_d(443)	a_{CDOM}(443)
pH	1	0.12 *	-0.26 **	0.05	-0.27 **	0.001	-0.16 **	0.02	-0.30 **	-0.13 *	-0.30**	-0.003
EC (μS cm^{-1})		1	-0.24 **	0.28 **	-0.23 **	-0.18 **	0.16 **	0.26**	-0.31 **	-0.21 **	-0.27**	-0.21 **
Turbidity (NTU)			1	-0.57 **	0.92 **	0.21 **	0.02	0.09	0.81 **	0.37 **	0.80**	0.30 **
SDD (m)				1	-0.58 **	-0.34 **	-0.10	-0.19**	-0.57 **	-0.42 **	-.491**	-0.47 **
SPM (mg L^{-1})					1	0.23 **	0.06	0.08	0.82 **	0.40 **	.805**	0.30 **
Chl-a (μg L^{-1})						1	0.32 **	0.05	0.41 **	0.71 **	.134*	0.47 **

TN (mg L^{-1})	1	0.20 **	0.11	0.28 **	-0.015	0.22 **
TP (mg L^{-1})		1	-0.02	0.06	-0.049	0.13 *
a(443) (m^{-1})			1	0.60 **	0.915 **	0.37 **
a_{ph}(443) (m^{-1})				1	0.229 **	0.58 **
a_d(443) (m^{-1})					1	0.16 **
a_g(443) (m^{-1})						1

* $p < 0.05$, ** $p < 0.01$.

Table S5. The Sentinel-2 A/B Level1C images used to estimate turbidity concentration in typical lakes.

Lake names	Sentinel-2 imagery
Chagan Lake	S2B_MSIL1C_20200418T023549_N0209_R089_T51TXL S2A_MSIL1C_20200725T024551_N0209_R132_T51TWL S2A_MSIL1C_20200930T023551_N0209_R089_T51TXL
Hulun Lake	S2B_MSIL1C_20200510T031539_N0209_R118_T50UNV S2A_MSIL1C_20200601T030551_N0209_R075_T50UMV S2A_MSIL1C_20200929T030551_N0209_R075_T50UNU
Taihu Lake	S2B_MSIL1C_20200428T023549_N0209_R089_T51RTQ S2A_MSIL1C_20200801T023551_N0209_R089_T51RTQ S2A_MSIL1C_20201109T023931_N0209_R089_T51RTQ
Qinghai Lake	S2A_MSIL1C_20200430T040551_N0209_R047_T47SPB S2A_MSIL1C_20200828T040551_N0209_R047_T47SPB S2B_MSIL1C_20201111T041009_N0209_R047_T47SPB
Dianchi	S2A_MSIL1C_20200511T033541_N0209_R061_T48RTN S2A_MSIL1C_20190815T033541_N0208_R061_T48RTN S2B_MSIL1C_20201013T033709_N0209_R061_T48RTN

Table S6. The description statistic and ANOVA analysis of water quality parameters considering different OWTs.

Parameters	OWT C1 (N=115)	OWT C2 (N=245)	OWT C3 (N=124)	ANOVA	
	average ± SD	average ±SD	average ±SD	F	p
pH	9.0 ± 1.1	7.4 ± 1.1	8.2 ±0.7	18.95	0.000
EC (μS cm^{-1})	4456.3 ± 6254.3	3472.4 ± 8180.7	1830.4 ± 3688.3	4.66	0.000
Turbidity (NTU)	8.8 ± 11.7	5.2 ± 7.5	92.93 ± 46.30	243.55	0.000
SDD (m)	1.7 ± 1.5	2.3 ± 1.5	0.4 ± 0.4	86.72	0.000
Chl-a (μg L^{-1})	6.1 ± 8.2	7.3 ± 13.9	9.2 ± 8.4	2.17	0.116
TP (mg L^{-1})	0.099 ± 0.3	0.067 ± 0.1	0.36 ± 0.7	22.39	0.000
SPM (mg L^{-1})	8.9 ± 8.8	4.9 ± 6.1	43.2 ± 23.2	361.32	0.000
a_{ph}(443) (m^{-1})	0.40 ± 0.53	0.32 ± 0.70	0.81 ± 0.77	20.60	0.000
a_d(443) (m^{-1})	0.38 ± 0.52	0.30 ± 0.48	2.43 ± 1.85	170.43	0.000
a_{CDOM}(443) (m^{-1})	0.45 ± 0.40	0.48 ± 0.40	0.71 ± 0.5	14.96	0.000

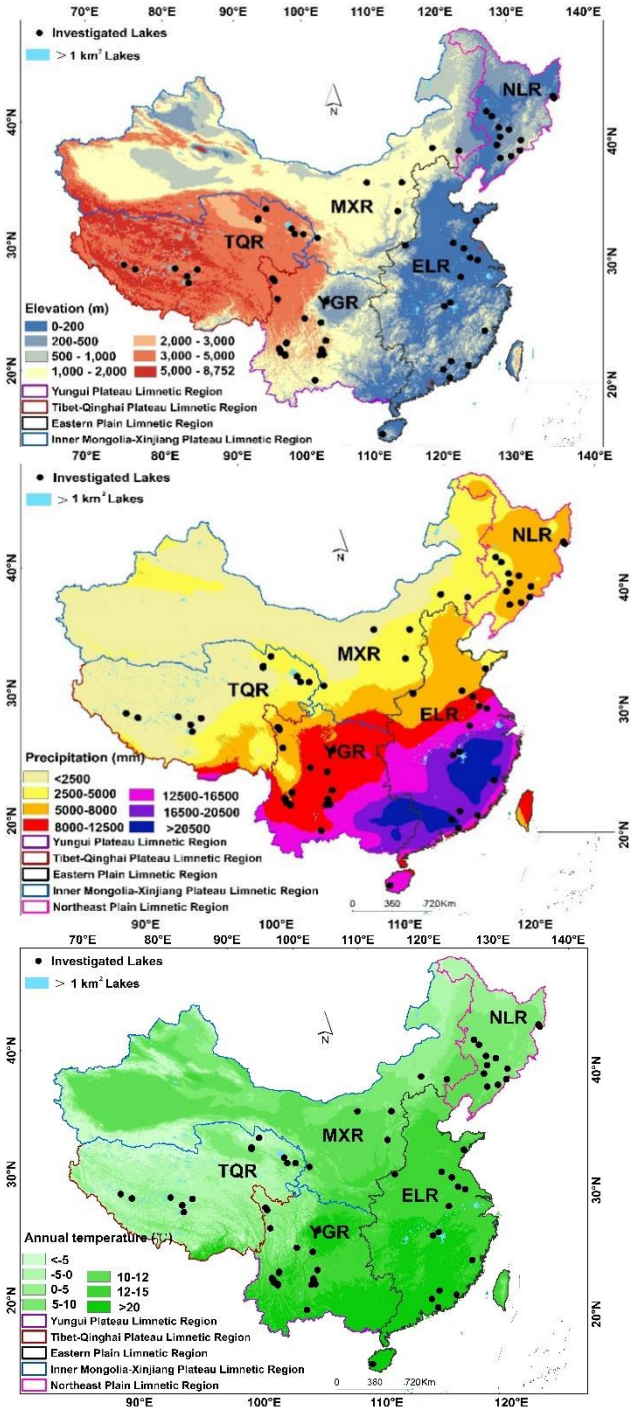
70°E
80°E
90°E
100°E
110°E
120°E
130°E
140°E
Investigated Lakes
> 1 km² Lakes
NLR
MXR
TQR
ELR
YGR
40°N
30°N
20°N
Elevation (m)
0-200
200-500
500 - 1,000
1,000 - 2,000
2,000 - 3,000
3,000 - 5,000
5,000 - 8,752
Yungui Plateau Limnetic Region
Tibet-Qinghai Plateau Limnetic Region
Eastern Plain Limnetic Region
Inner Mongolia-Xinjiang Plateau Limnetic Region
Precipitation (mm)
<2500
2500-5000
5000-8000
8000-12500
12500-16500
16500-20500
>20500
Northeast Plain Limnetic Region
0 360 720Km
Annual temperature (℃)
<-5
-5-0
0-5
5-10
10-12
12-15
>20

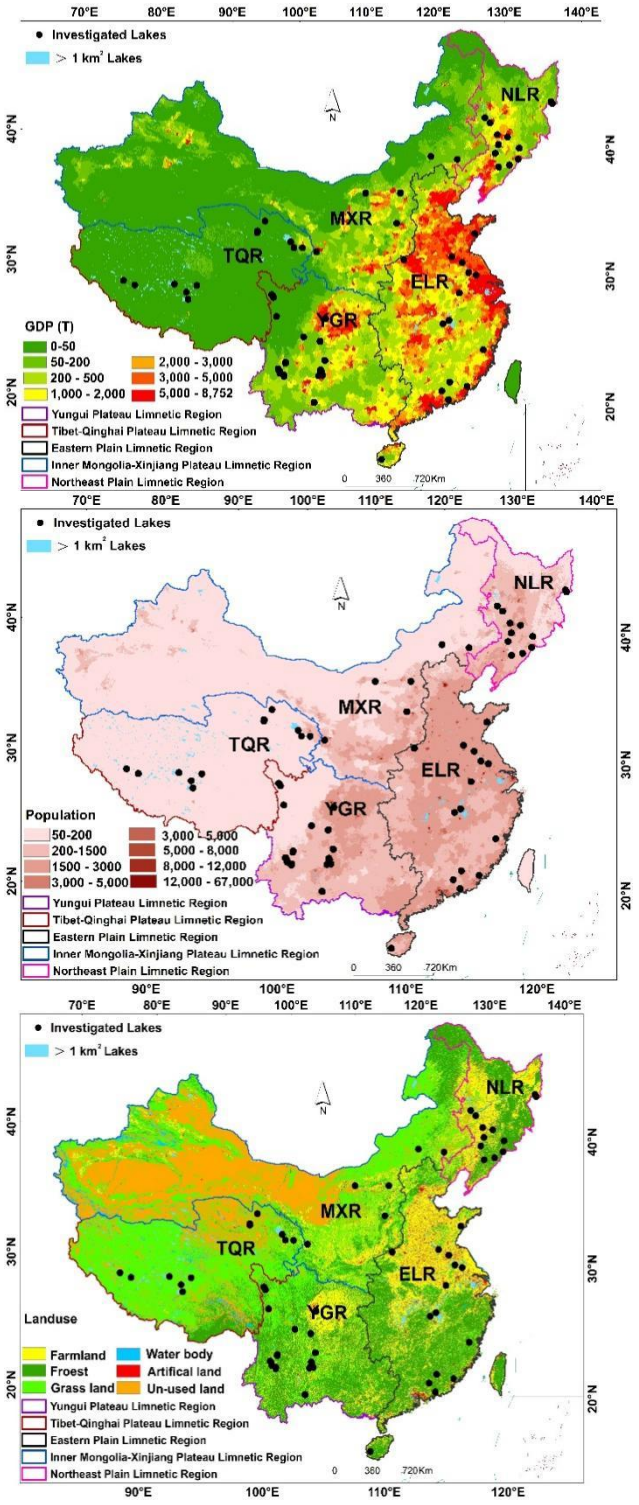

Figure S1. The DEM, temperature and precipitation GDP, population and land-use distribution maps of China.

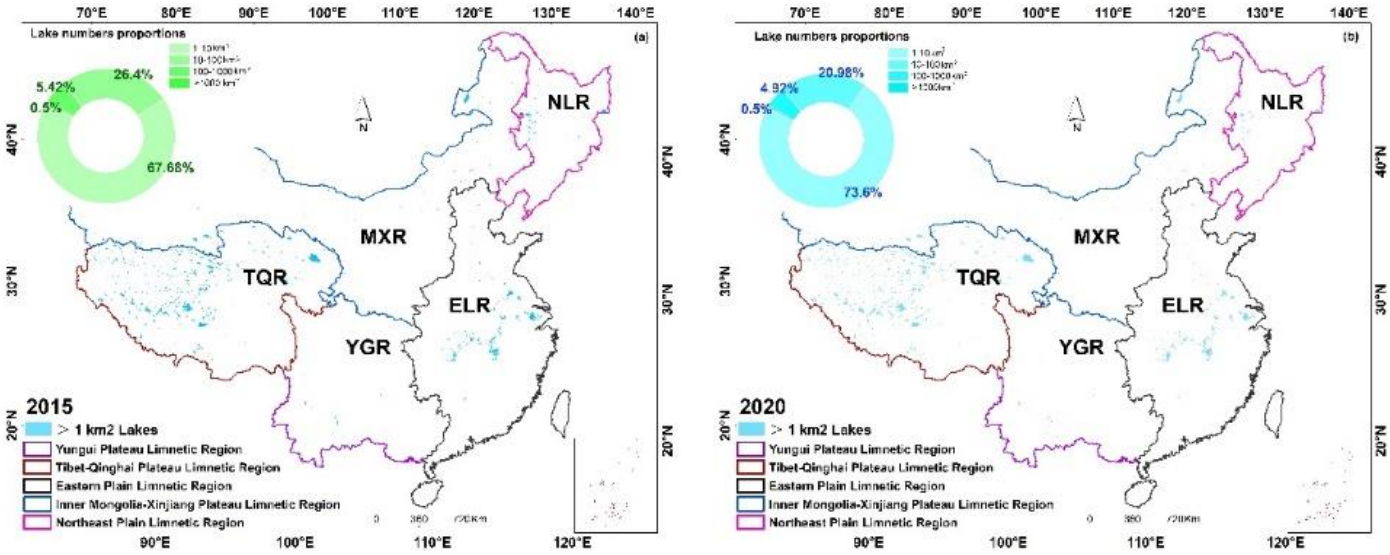

Figure S2. Chinese lake numbers distributions and proportions in 2015 (a) and 2020 (b). The data from Zhang et al., (2019) and lake boundaries (1960s-2020) have been released by the National Tibetan Plateau Data Centre. The lake area proportions were calculated and shown in ring graphs in 2015 (a, green) and 2020 (b, blue) considering four area levels, i.e., 1-10 km^2, 10-100km^2, 100-1000 km^2 and >1000 km^2.

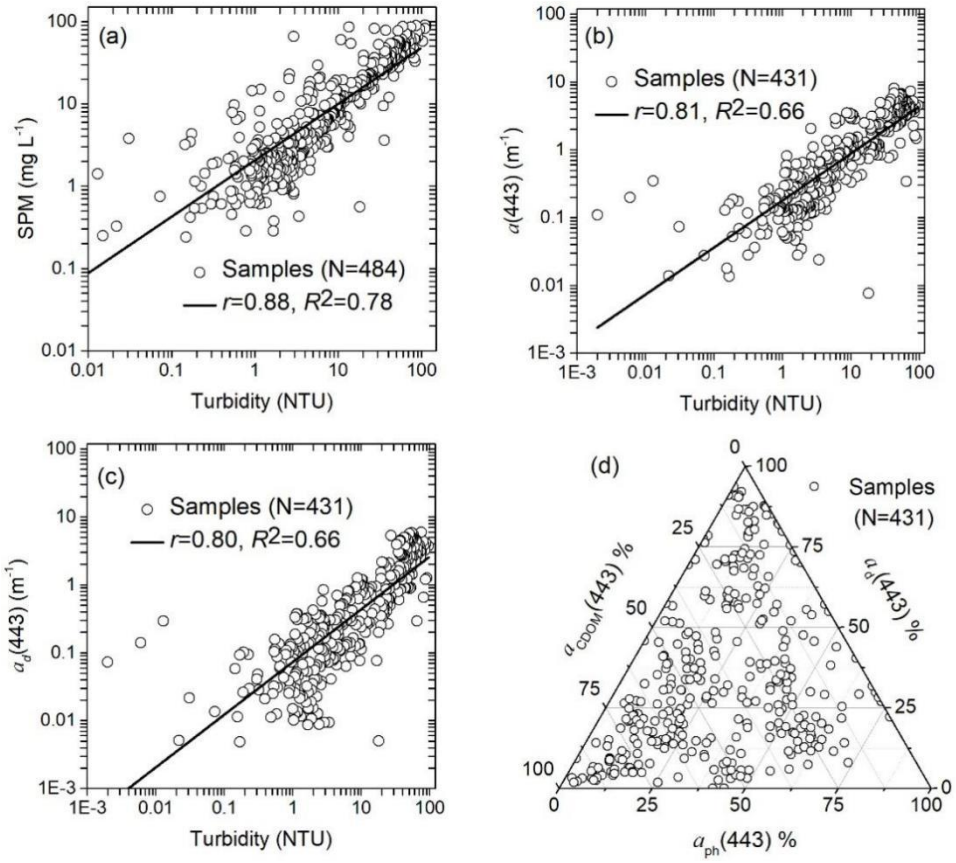

Figure S3. The regression analysis of turbidity and SPM (**a**), a(443) (**b**) and a_d(443) (**c**), and the absorption contribution at 443 nm of phytoplankton pigment absorption a_{ph}(443), non-algal particles a_d(443) and CDOM absorption a_{CDOM}(443) (**d**). The r is Pearson correlation coefficients found in Table S1, and R^2 is regression coefficient, respectively.

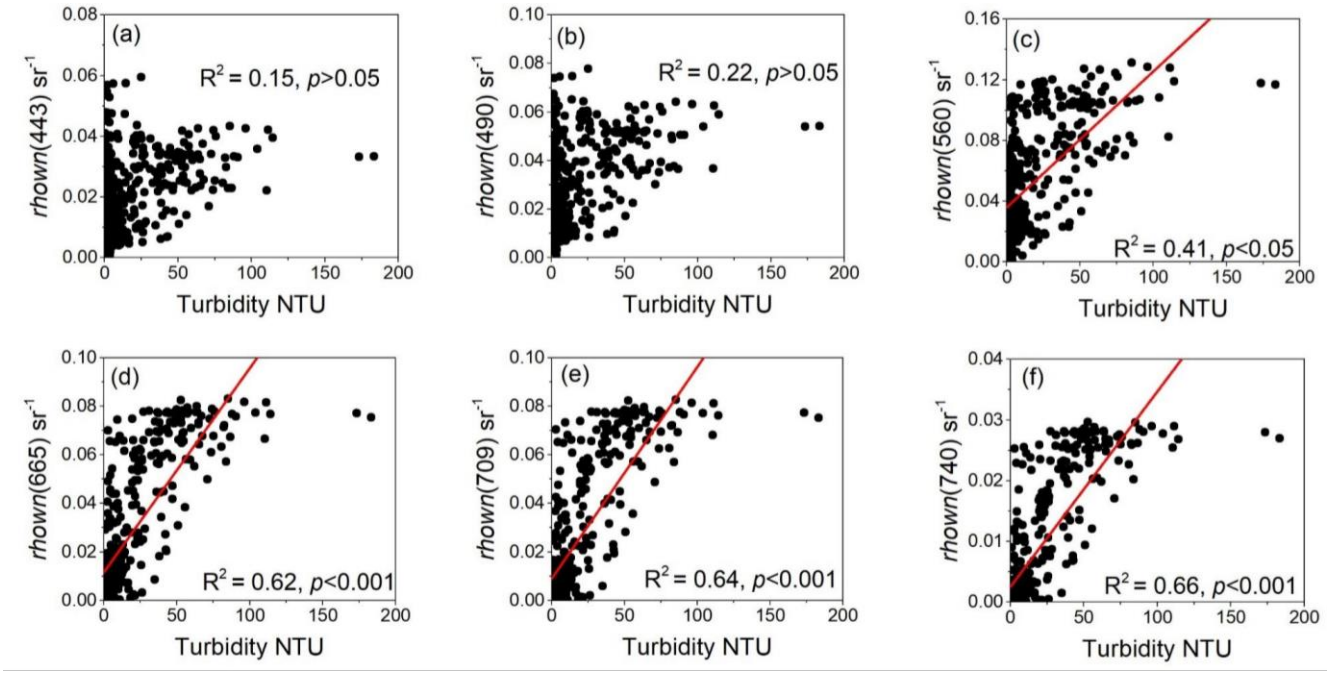

Figure S4. The regression analysis of *rhown*(λ) and turbidity, (**a**) *rhown*(443), (**b**) *rhown*(490), (**c**) *rhown*(560), (**d**) *rhown*(665), (**e**) *rhown*(709) and (**f**) *rhown*(740), for all data sets. The R^2 is regression coefficient, respectively. .

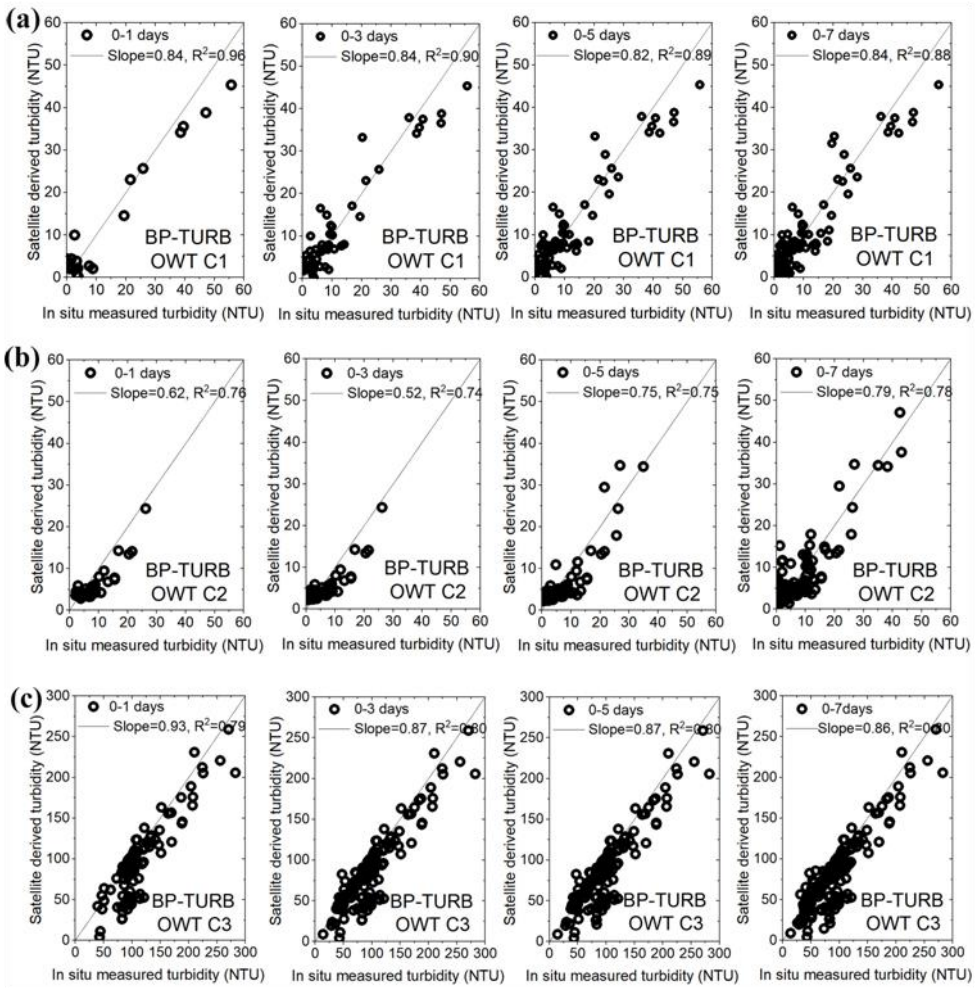

Figure S5. The performance of BP-TURB model considering different time-window, e.g., 0-1 days, 0-3 days, 0-5 days and 0-7days with different BP-TURB algorithms evaluation (**a**), BP OWT-C1; (**b**), BP OWT-C2; (**c**) BP OWT-C3).